Sensors and Materials, Vol. 35, No. 7 (2023) 2355–2370
MYU Tokyo

S & M 3327

Convolutional Takagi–Sugeno–Kang-type Fuzzy Neural Network for Bearing Fault Diagnosis

Jyun-Yu Jhang,[1] Cheng-Jian Lin,[2*] and Su-Wei Kuo[2]

[1]Department of Computer Science and Information Engineering,
National Taichung University of Science and Technology, Taichung 404, Taiwan
[2]Department of Computer Science & Information Engineering, National Chin-Yi University of Technology,
Taichung 411, Taiwan

(Received April 7, 2023; accepted June 27, 2023)

Keywords: fault diagnosis, deep learning network, Takagi–Sugeno–Kang (TSK)-type fuzzy neural network, vibration signal

Rotating machines are widely used in modern industry. In a mechanical system, rolling bearings are essential. Bearings must be able to operate in extreme environments, in which they are prone to various faults. To address the challenge related to accurately classify bearing fault types using vibration sensors, we propose a convolutional Takagi–Sugeno–Kang (TSK)-type fuzzy neural network classifier (CTFNNC) that comprises a convolutional layer and a TSK-type fuzzy neural network. In the CTFNNC, convolutional layers are used to extract the features of a vibration signal, and a TSK-type fuzzy neural network is used to classify bearing faults under various categories. In our experiment, the proposed CTFNNC was compared with other methods, such as a fuzzy neural network, an artificial neural network, and the LeNet-5 convolutional neural network. The experimental results indicate that the proposed CTFNNC has a bearing fault classification accuracy of 98.3% and requires half the number of parameters as LeNet-5.

1. Introduction

Because of the rapid development of the modern manufacturing industry, the reliability, safety, and availability of mechanical systems are increasingly being studied.[1,2] Rolling bearings are among the most widely used components in machines and the most common cause of machine failure.[3] Approximately 30% of all machine failures, especially those that occur in gear- and shaft-driven equipment, are related to bearings.[4] During the operation of equipment, its bearings are susceptible to overload, friction, corrosion, and sticking damage, which are likely to affect the performance of the equipment and may even cause personal injury. An instant and accurate bearing fault diagnosis system is required to ensure machine performance. Traditional bearing fault diagnosis systems mostly rely on the analysis of bearing vibration signals using vibration sensors, which is performed by empirical mode decomposition (EMD) or ensemble empirical mode decomposition (EEMD). EMD decomposes a signal into multiple

*Corresponding author: e-mail: cjlin@ncut.edu.tw
https://doi.org/10.18494/SAM4440

ISSN 0914-4935

signal features through an adaptive method, which has achieved excellent results in bearing fault diagnosis.[5–9] EEMD is a data analysis technique that uses noise to address the shortcomings associated with the common-mode mixing effect of EMD and is widely used to diagnose gear spalling and cracking faults.[10–12] EEMD identifies different fault problems on the basis of fault signals. Therefore, fault diagnosis-related problems can be regarded as classification problems.

Machine learning for classification problems has been widely used in human recognition, speech recognition, and fault detection. Many mature machine learning methods exist for fault diagnosis classification, such as the fuzzy logic system (FLS), artificial neural network (ANN), fuzzy neural network (FNN), and support vector machine (SVM). To diagnose faults, Goddu *et al.*[13] employed a fuzzy logic technique to analyze the frequency spectrum of bearing vibration signals. They used a hand-optimized method to design membership functions, and their preliminary results indicated that fuzzy logic can be effectively utilized to obtain highly accurate bearing fault diagnosis results. To improve the performance of the FLS and its compatibility with complex systems, Bin and Wenbo[14] used the Takagi–Sugeno–Kang (TSK) fuzzy inference system, which is a modified Sugeno fuzzy inference system that employs a different approach to manage its rule base and output. The TSK system is recognized for its ability to manage nonlinear systems and to provide more accurate and precise outputs than other fuzzy inference systems. Wang *et al.*[15] proposed a new TSK fuzzy broad learning system model that combines the advantages of both broad learning systems and fuzzy systems, and it has produced favorable results with respect to both experimental accuracy and training time. Patil *et al.*[16] developed a method based on the wavelet transform and ANNs to analyze the vibration signals of rolling bearings and to identify component defects. In the method, a vibration signal is processed using the wavelet transform to remove noise and extract relevant features. These features include skewness, kurtosis, root mean square, and crest factor, which are retrieved as parameters that are input into an ANN classifier. The role of an ANN is to classify the bearing fault features generated by the wavelet transform and to identify the bearing faults. Experimental results indicated that the proposed method combining the wavelet transform and ANNs enables highly accurate and reliable bearing fault detection and classification. An FNN is an artificial intelligence model combining the characteristics of fuzzy logic systems and neural networks. It processes uncertain and imprecise input data and performs complex nonlinear tasks such as modeling and decision-making. The fuzzy logic aspect of an FNN is mainly used to preprocess input data and create fuzzy rules that support neural network training. By contrast, the neural network of an FNN is responsible for learning the underlying relationship between inputs and outputs and making predictions on the basis of a learned model. FNNs have been applied in various areas, such as control systems, pattern recognition, time series forecasting, and classification. Gai and Hu[17] developed a system for diagnosing crankshaft bearing failures in diesel engines. First, they decomposed the vibration signal of a crankshaft bearing in a known state by EMD to obtain the modal component of the fault characteristic information. Subsequently, they subjected the modal components of identified fault characteristics to singular value decomposition to generate a fault feature matrix, which was then classified by an FNN to identify and diagnose various crankshaft bearing conditions. Wang *et al.*[18] used integrated fault features (IFFs) and SVMs to achieve rapid, high-precision fault detection. They obtained the

feature information of a fault by separating IFF signals using EMD. Subsequently, an SVM was used to classify the fault features to detect the fault type. The aforementioned methods are all machine-learning-based methods. Although machine learning can be applied to effectively establish classification models on the basis of feature information, machine-learning-based methods require experts to design feature extraction methods, and poorly extracted feature information leads to poor classification performance.

In recent years, the performance of computing equipment has substantially improved, and deep learning has replaced machine learning as the most widely used method. Deep learning is a subfield of machine learning, and it involves training ANNs with multiple layers to learn and represent complex patterns in data. It allows a network to automatically learn and extract features from raw input data instead of through manual feature engineering.[19,20] Thus, it is suitable for tasks such as image and speech recognition, natural language processing, and self-driving. The key advantage of deep learning is its ability to effectively generalize the use of new examples and to learn from unstructured data. Li *et al.*[21] proposed an improved LeNet-5 convolutional neural network (CNN) for diagnosing rolling bearing faults. This CNN is a modified version of the conventional LeNet-5 model that incorporates additional convolutional layers and pooling layers. It uses convolutional layers to extract the features in a fault signal and then uses a *softmax function* to classify and identify rolling bearing faults. Wang *et al.*[22] devised a new method for fusing multimodal sensor signals (e.g., vibration signals from accelerometers and audio signals from microphones) to increase the accuracy and robustness of bearing fault diagnosis. Their proposed method uses 1D CNN-based networks to merge features extracted from raw vibration signals and acoustic signals, and it provides higher accuracy than traditional methods. Lin and Jhang[23] used a gradient-weighted class activation map (Grad-CAM)-based convolutional neuro-fuzzy network to detect the bearing conditions of machine tools. They analyzed the characteristics of multiple fault signals through the visualization technology of Grad-CAM and established a classification model by using a convolutional neuro-fuzzy network. Their implementation results revealed that the prediction accuracy of their method was higher than that of the traditional CNN method. Hasan *et al.*[24] combined a 1D CNN with the transfer learning method to solve deep learning problems that require a long training time. The proposed method used the information obtained under a given operating condition to diagnose faults occurring under other operating conditions.

Although deep learning methods can be effectively applied to establish fault prediction models, quickly importing them into industrial applications is challenging because they require considerable computing resources and a long training time. Therefore, in this study, we propose a novel convolutional TSK-type FNN classifier (CTFNNC) for bearing fault diagnosis that uses convolution operations to extract features from faulty signals. The main contributions of this study are as follows:

1. The proposed CTFNNC can automatically extract features from raw data without requiring expert knowledge.
2. In the proposed CTFNNC, a TSK-type FNN (TSK-FNN) is used to replace a fully connected network as classifier. The extracted feature information is used as the input for the TSK-FNN to build a fault diagnosis model.

3. Compared with the fully connected network used by a traditional CNN, the proposed CTFNNC uses fewer training parameters and has powerful nonlinear mapping capabilities, which improve the accuracy and reduce the training time.
4. By comparing the experimental results of the proposed method with those of four other methods, we verified that the CTFNNC requires half the number of parameters (12K) as a traditional CNN (24K) and achieves high accuracy (98.6%).

The remainder of the paper is organized as follows. Section 2 presents the system architecture used for fault diagnosis and the data preprocessing steps. Section 3 introduces the experimental data set and experimental results. Section 4 provides the conclusion.

2. Proposed CTFNNC for Bearing Fault Diagnosis

2.1 System architecture

Figure 1 presents a structural diagram of the bearing fault detection system proposed in this study. The system detects bearing faults by (1) dividing the original signal of a data set into several subsample sets with a length of 1024, (2) converting the signal of the subsample set into a 2D vibration image map, (3) converting the vibration image set to train the CTFNNC to establish a bearing fault diagnosis model, and (4) outputting the classification of 16 states, including the normal (Normal), inner race damage (DEIR_007, DEIR_014, DEIR_021, DEIR_028), ball damage (DEB_007, DEB_014, DEB_021, DEB_028), and outer race damage (DEOR@6, DEOR@3, DEOR@12) states.

2.2 Data preprocessing

In this study, the 12K vibration signals obtained using a vibration sensor in the Case Western Reserve University (CWRU) bearing database were adopted to establish a bearing fault diagnosis model. First, each vibration signal was split into several non-overlapping subsignals with a sample size of 1024. Subsequently, each subsignal with a size of 1024 was converted into a 32 × 32 vibration image, which was then used as the training and testing data of the diagnostic

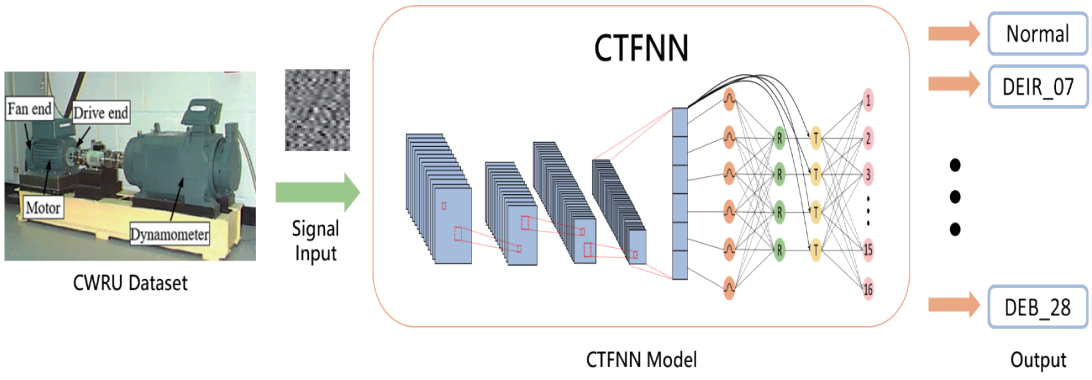

Fig. 1. (Color online) Structure of bearing fault detection system.

model (Fig. 2). The bearing data set contained four states, namely, the normal, inner race fault, ball damage, and outer race fault states. The total numbers of samples used for the normal, inner race fault, ball fault, and outer race fault states were 1656, 1893, 1893, and 3324, respectively. Figure 3 shows 2D images of various fault states.

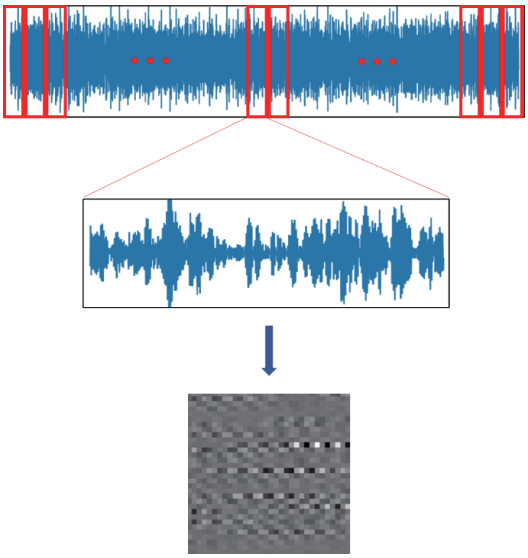

Fig. 2. (Color online) Process of converting vibration signal into vibration image.

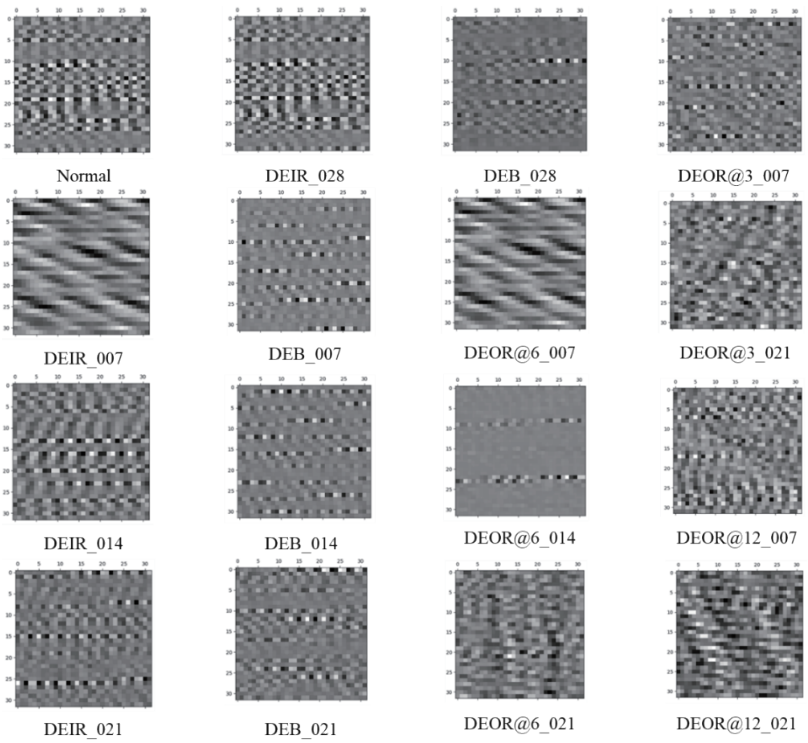

Fig. 3. Two-dimensional images of various fault states.

2.3 CTFNNC

To improve the use of fully connected networks in traditional CNNs, numerous network parameters and a long training time are required. In this study, we propose a novel CTFNNC for establishing a bearing fault diagnosis model. The proposed CTFNNC comprises seven layers, namely, the convolutional layer, pooling layer, flattening layer, fuzzification layer, rule layer, TSK layer, and output layer (Fig. 4). The operation of each layer is described in the subsequent subsections.

(1) Convolutional layer

The convolution layer is among the most crucial cores in a CNN; it mainly extracts features from an input image using several convolution kernels.[25] In general, each filter extracts one type of feature, and different filters extract different features. During forward propagation, each filter is convoluted with an input feature map, and through the convolution operation, a new feature map is generated as the input of the next layer. The formula expressing the convolution operation is

$$C_{ri} = \sum_{y=1}^{m-1} C_{i+y} \otimes K_{(r,y)}, \tag{1}$$

where $\otimes$ is the convolution operation symbol, C_{i+y} represents the input data, m is the size of the convolution kernel, and $K_{(r, y)}$ represents the convolution kernel of position (r, y).

(2) Pooling layer

The pooling layer in the CNN architecture compresses the feature map after a convolution operation is performed, thereby reducing the number of network parameters required. A max pooling operation requires the selection of a kernel size and a stride, thereby allowing a kernel to slide over the input with the specified stride. Only the maximum value of each kernel is selected from the input to produce the output value. The output formula of the max pooling operation is as follows:

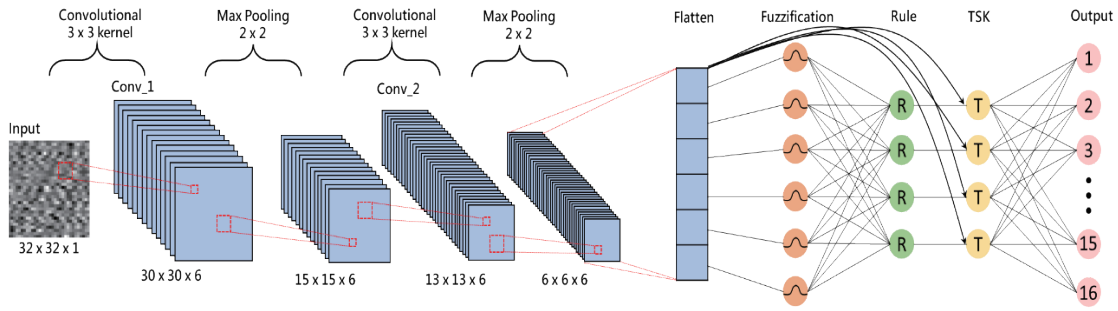

Fig. 4. (Color online) Architecture of convolutional TSK-type FNN classifier.

$$P_{rj} = \max C_{ri}, \tag{2}$$

where $P_i^{(k)}$ is the feature map produced through the max pooling operation.

(3) Flattening layer

The 2D feature map generated after the convolution and max pooling operations is converted into a 1D feature vector by using the flattening layer as the input of the classifier. The formula for expressing a flattening operation is as follows:

$$P_{rj} \rightarrow U_i,\ i = r \times n + j\ , \tag{3}$$

where U_i represents the 1D vector at position i, P_{rj} represents the feature map generated by the pooling operation, and n is the total number of rows of the feature map.

(4) Fuzzification layer

The fuzzification layer uses the IF~THEN~ rules for fuzzification. The fuzzy rules IF~THEN~ are as follows:

$$\begin{gathered}\text{IF } U_1 \text{ is } S_{k1} \text{ and } U_2 \text{ is } S_{k2} \text{ and } \ldots \text{ and } U_j \text{ is } S_{kj} \text{ and } \ldots \text{ and } U_n \text{ is } S_{kn} \\ \text{THEN } y_k = c_{0k} + c_{1k}U_1 + c_{2k}U_2 + \ldots + c_{jk}U_j + \ldots + c_{nk}U_n,\end{gathered}$$

where S_{kj} is the antecedent fuzzy set of the kth fuzzy rule and c_{jk} is the parameter of the TSK consequences. In this study, the Gaussian function[26] was used as the membership function, and the formula is presented as

$$\mu_{kj}(U) = \exp\left(-\frac{1}{2}\left(\frac{U_j - C_{kj}}{\sigma_{kj}}\right)\right), \tag{4}$$

where C_{kj} and σ_{kj} are the mean and standard deviation of the Gaussian fuzzy set, respectively.

(5) Rule layer

The firing strength of the fuzzy rules is obtained by multiplying each membership function, and the algebraic product operation is expressed as

$$\mu_k(U) = \prod_{j=1}^{n} \mu_{kj}(U_j). \tag{5}$$

(6) TSK layer

In this paper, TSK is used as the consequence of the fuzzy rule. The TSK consequence is defined as

$$t_k = \mu_k(U)\left(c_{0k} + \sum_{i=1}^{n} c_{ik}U_i\right). \tag{6}$$

(7) Output layer

Finally, a defuzzification operation is performed through the center of gravity method as follows:

$$y = \sum_{k=1}^{r} \frac{t_k}{\sum_{k=1}^{r} \mu_k(U)}. \tag{7}$$

3. Experimental Results

3.1 CWRU bearing data set

Bearings naturally deteriorate over many years. Therefore, collecting data on bearing failures is challenging. To collect experimental data on bearing defects, artificial methods are usually used to accelerate the generation of bearing defect data.[27] Numerous research centers have publicly shared the bearing data sets that they have collected, including the CWRU bearing data set,[28] NASA intelligent maintenance system data set,[29] Paderborn University bearing data set,[30] and PRONOSTIA bearing data set,[31] among which the CWRU bearing data set is the most widely used benchmark.[32,33] In this study, the CWRU bearing data set was adopted to develop a bearing fault diagnosis model. Figure 5 presents the experimental machine used to

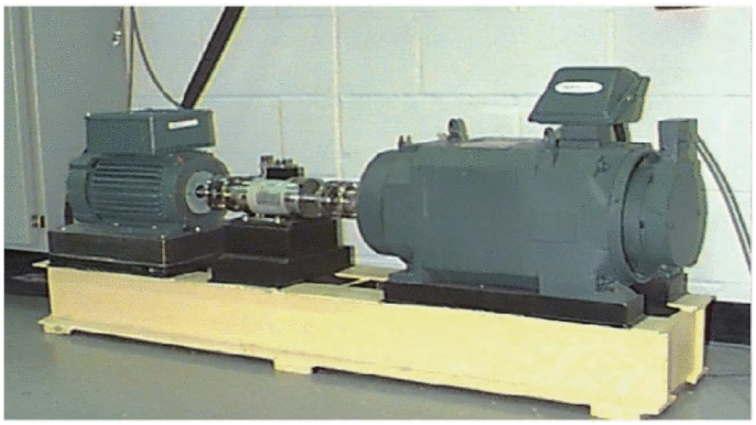

Fig. 5. (Color online) Experimental machine used to generate CWRU bearing data set.

generate the data of the CWRU bearing data set. This machine has three components. The first component is a 2 horsepower (hp) electric motor that runs at a constant speed, the second is a torque sensor/encoder that collects speed and horsepower data, and the third is an accelerometer that collects bearing vibration data.

The CWRU bearing data set comprises four states, namely, the normal, inner race fault, ball fault, and outer race fault states. The sampling rates of the data set are 12 and 48 kHz, and vibration signals are collected under 0, 1, 2, and 3 hp loads. The diameters of the ball bearings are 0, 0.007, 0.014, 0.021, and 0.028, respectively. The motor speeds corresponding to the loads of 0, 1, 2, and 3 hp are 1797, 1772, 1750, and 1730 rpm, respectively. The outer race fault state is different from the other three fault states and is classified into centered, orthogonal, and opposite outer race faults. These three race faults are at the 6 o'clock (@6), 3 o'clock (@3), and 12 o'clock (@12) positions, respectively. In the present experiment, vibration data with a sampling frequency of 12 kHz were used without considering the motor load and speed. For example, all inner race faults with a diameter of 0.007 are considered as the same fault type, regardless of the motor load and speed. The conditions corresponding to various bearing vibration signals are presented in Table 1, where the symbol "-" indicates the absence of data. The 16 status conditions are labeled as Normal, DEIR_007, DEIR_014, DEIR_021, DEIR_028, DEB_007, DEB_014, DEB_021, DEB_028, DEOR@6_007, DEOR@6_014, DEOR@6_021, DEOR@3_007, DEOR@3_021, DEOR@12_007, and DEOR@12_021. Table 2 lists the number of records for various bearing faults.

Table 1
Fault labels corresponding to various bearing vibration signals.

Fault diameter	Motor load	Motor speed	Normal	Inner race	Ball	Outer race (Fault position)		
						@6	@3	@12
0	0	1797	Normal	—	—	—	—	—
	1	1772						
	2	1750						
	3	1730						
0.007	0	1797	—	DEIR_007	DEB_007	DEOR@6_007	DEOR@3_007	DEOR@12_007
	1	1772						
	2	1750						
	3	1730						
0.014	0	1797	—	DEIR_014	DEB_014	DEOR@6_014	—	—
	1	1772						
	2	1750						
	3	1730						
0.021	0	1797	—	DEIR_021	DEB_021	DEOR@6_021	DEOR@3_021	DEOR@12_021
	1	1772						
	2	1750						
	3	1730						
0.028	0	1797	—	DEIR_028	DEB_028	—	—	—
	1	1772						
	2	1750						
	3	1730						

Table 2
Number of records for each failure type.

Fault diameter	Normal	Inner race	Ball	Outer race (Fault position)		
				@6	@3	@12
0	1656	—	—	—	—	—
0.007	—	476	473	475	474	476
0.014	—	472	475	474	—	—
0.021	—	474	475	476	475	474
0.028	—	471	471	—	—	—

3.2 Bearing fault diagnosis and evaluation experiment

We compared the proposed CTFNNC model with several machine learning or deep learning models to evaluate its diagnostic performance. Chang[34] proposed an FNN-based diagnostic technique, Ogi *et al.* [35] proposed an ANN for gas insulated switchgear (GIS) diagnostic system application, Li *et al.*[36] improved LeNet-5 for rolling bearing fault diagnosis, and Lin *et al.*[37] proposed a convolutional fuzzy neural network (CFNN) for use in intelligent traffic-monitoring systems. To clearly present the differences in the classification performance of various models, we used a confusion matrix[38] to evaluate the performance of the proposed classification model for bearing fault diagnosis compared with those in Refs. 34–37. Table 3 provides a comparison of the accuracy of the proposed CTFNNC with those of the other models. After 10 epochs of training, the lowest, highest, and average accuracies were obtained. The average accuracies of the FNN, ANN, CFNN, and LeNet-5 models were 60.15, 62.94, 96.34, and 96.68%, respectively (Table 3). The proposed CTFNNC outperformed these methods in terms of the lowest (98.37%), highest (98.86%), and average (98.6%) accuracies. For the evaluation of network parameters, the proposed CTFNNC used approximately half the number of parameters as that used by the traditional CNN (LeNet-5).

Table 4 lists the accuracy results obtained under normal and inner race fault conditions, revealing that the accuracy for normal bearing diagnosis was 100% for each model, whereas that for inner race failure was significantly different among the models. In addition, the diagnostic accuracies of the FNN and ANN were low because they did not use a convolutional layer to extract features.

Table 5 lists the accuracy results for various ball fault sizes. The proposed method accurately classified ball faults, especially the DEB_014 and DEB_028 fault types, with accuracies of 95.80 and 100%, respectively. The classification accuracy of the FNN for DEB_014 was approximately 20% and that of the ANN for DEB_028 was nearly 40%.

Table 6 lists the accuracy results for outer race faults. Because each outer race fault was located at the 6 o'clock position, it is denoted as @6. Table 6 reveals that the CFNN, LeNet-5, and proposed models exhibited similarly high diagnostic accuracies. However, the FNN and ANN exhibited poor accuracies for outer race fault detection.

Table 7 lists the accuracy results for the diagnosis of orthogonal outer race faults. Because the orthogonal outer race faults were located at the 3 o'clock and 12 o'clock positions, they are denoted as @3 and @12, respectively. Table 7 indicates that the CFNN, LeNet-5, and CTFNNC

Table 3
Accuracy of various methods for bearing fault diagnosis.

Classifiers	Lowest accuracy (%)	Highest accuracy (%)	Average accuracy (%)	Parameters
FNN[34]	58.53	63.66	60.15	66064
ANN[35]	59.06	65.72	62.94	68208
CFNN[37]	88.26	98.29	94.96	7574
LeNet-5[36]	95.86	98.06	96.68	23586
CTFNNC	98.37	98.86	98.6	12376

Table 4
Classification accuracy for normal and inner race faults.

Classifier	Normal (%)	DEIR_007 (%)	DEIR_014 (%)	DEIR_021 (%)	DEIR_028 (%)
FNN[34]	100.00	57.34	60.56	93.66	100.00
ANN[35]	100.00	37.06	50.00	61.27	58.87
CFNN[37]	100.00	100.00	97.89	100.00	100.00
LeNet-5[36]	100.00	99.30	92.25	100.00	99.29
CTFNNC	100.00	100.00	100.00	100.00	100.00

Table 5
Classification accuracy for ball faults.

Classifier	DEB_007 (%)	DEB_014 (%)	DEB_021 (%)	DEB_028 (%)
FNN[34]	85.21	20.28	69.23	100.00
ANN[35]	61.27	50.00	57.34	39.72
CFNN[37]	94.37	96.50	88.81	100.00
LeNet-5[36]	93.66	95.80	90.91	99.29
CTFNNC	93.66	95.80	93.01	100.00

Table 6
Classification accuracy for outer race faults.

Classifier	DEOR@6_007 (%)	DEOR@6_014 (%)	DEOR@6_021 (%)
FNN[34]	85.21	20.28	69.23
ANN[35]	61.27	50.00	57.34
CFNN[37]	94.37	96.50	88.81
LeNet-5[36]	93.66	95.80	90.91
CTFNNC	93.66	95.80	93.01

Table 7
Classification accuracy for orthogonal outer race faults.

Classifier	DEOR@3_007 (%)	DEOR@3_014 (%)	DEOR@12_007 (%)	DEOR@12_021 (%)
FNN[34]	0.00	32.87	78.32	16.20
ANN[35]	71.13	55.24	60.14	42.25
CFNN[37]	100.00	100.00	99.3	97.18
LeNet-5[36]	100.00	98.60	97.2	96.48
CTFNNC	100.00	100.00	98.6	97.89

models accurately diagnosed these fault types. However, the ANN and FNN achieved diagnostic accuracies of only about 60 and 80% for DEOR@12_007, respectively, which were much lower than the results for the other types of orthogonal outer race faults. Collectively, these findings indicate that without a convolutional layer to assist in feature extraction, traditional machine learning models cannot effectively classify fault states during fault diagnosis.

To identify the advantages and disadvantages of the models, confusion matrices were used to compare them. Because the FNN and ANN did not use convolutional layers to automatically extract features, only the CFNN, LeNet-5, and proposed CTFNNC were used for diagnosis. The confusion matrices (Fig. 6) revealed that the classification accuracies of these three models were lowest for the DEB_021 fault type. That is, the fault characteristics of DEB_021 and DEB_007 were similar, making it difficult for the CFNN and LeNet-5 models to accurately classify them. However, the accuracy of the proposed model for DEB_021 was 93.01%, higher than those of the CFNN and LeNet-5, whose accuracies were 88.81 and 90.91%, respectively. That is, the proposed method was superior to the other detection models and could effectively detect the state of bearings.

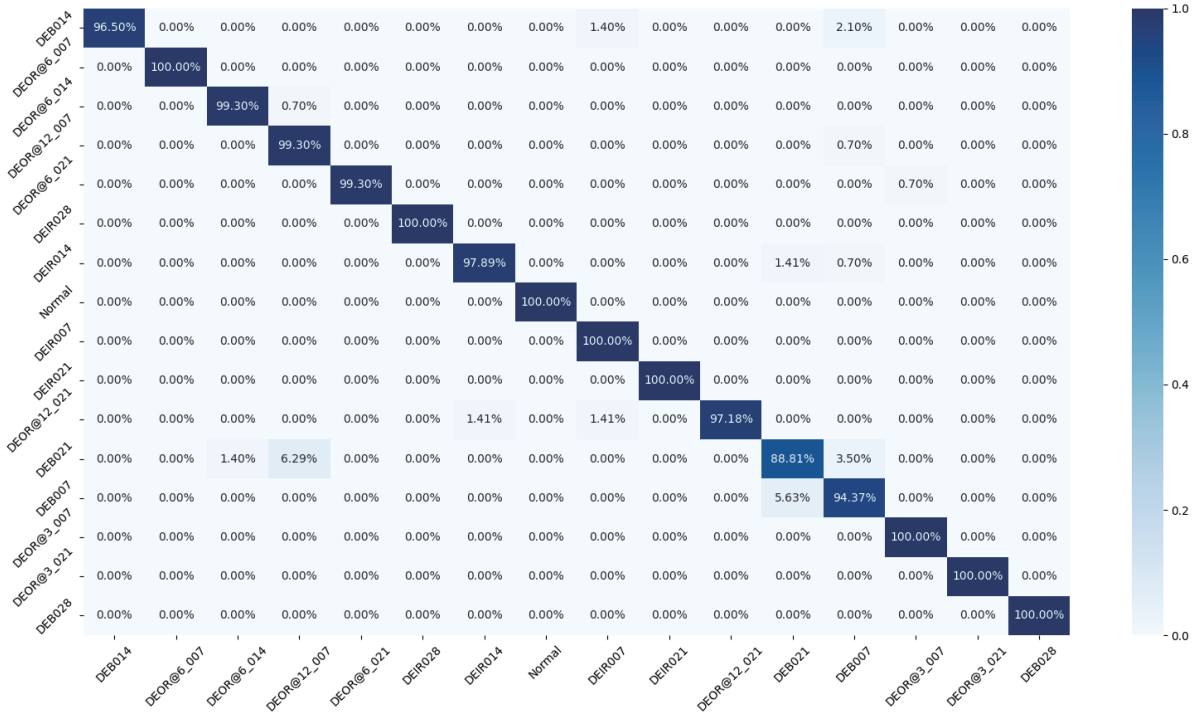

(a)

Fig. 6. (Color online) Confusion matrix of fault diagnosis models. (a) CFNN.

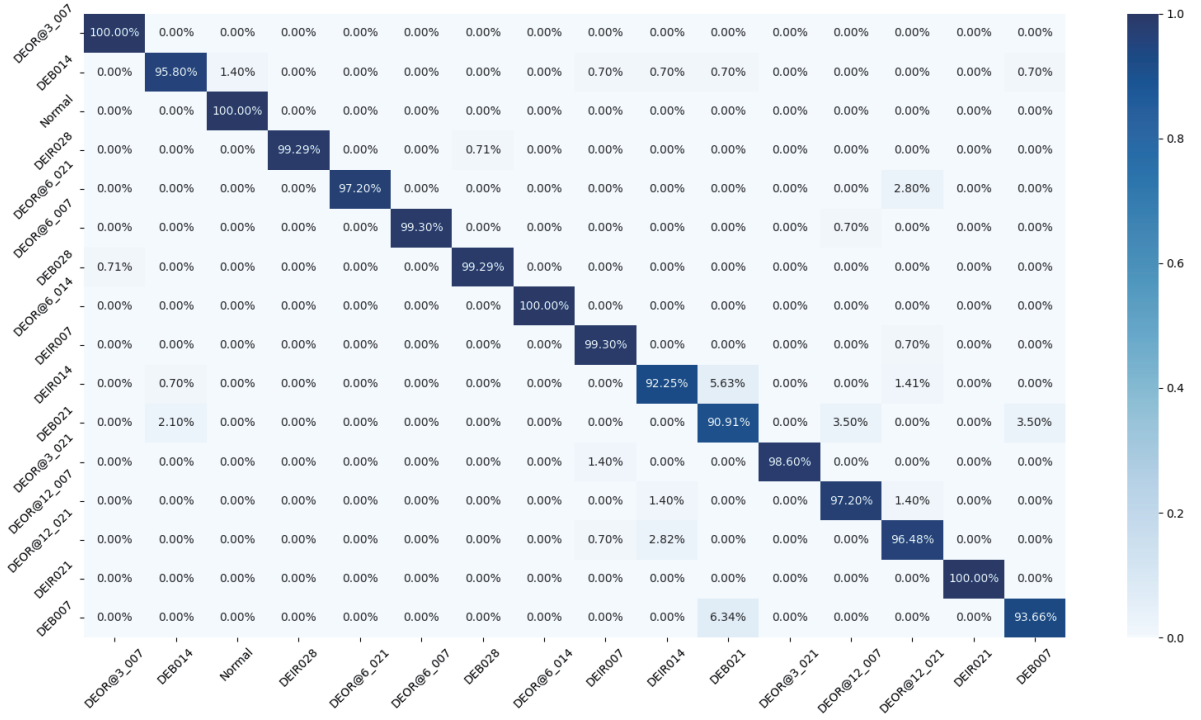

(b)

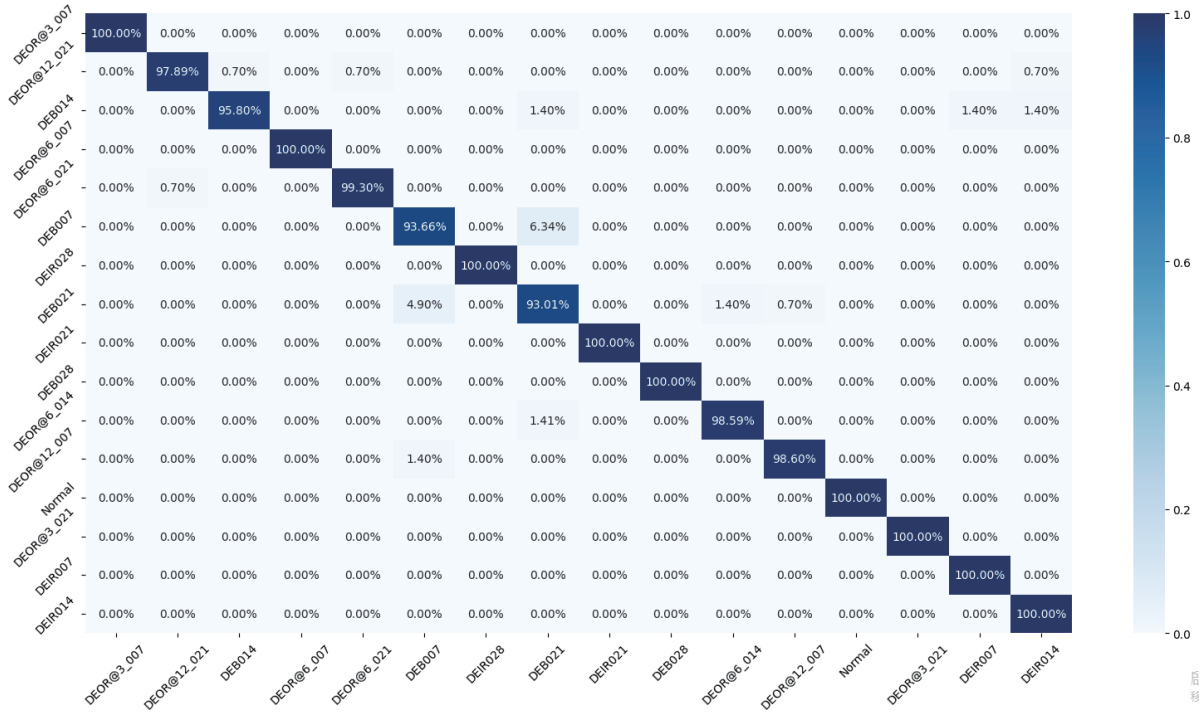

(c)

Fig. 6. (Continued) (Color online) (b) LeNet-5 and (c) proposed CTFNNC.

4. Conclusions

We proposed a CTFNNC for detecting the current state of a bearing signal from vibration sensors. Traditional feature extraction requires manual methods, for which the classification process is time-consuming. The proposed method can automatically perform feature extraction on the basis of raw vibration signals. Among the studied methods, the TSK-FNN effectively reduced the number of parameters used for training and improved the classification accuracy. By comparing the experimental results of the proposed method with those of the other four studied methods, we verified that the CTFNNC required half the number of parameters (12K) as a traditional CNN (24K) and achieved a high accuracy (98.6%). The experimental results indicate that the proposed method is effective and feasible for performing bearing fault diagnosis.

The bearing fault diagnosis system must be real-time in industrial applications. Therefore, the proposed CTFNNC can be implemented in field-programmable gate array (FPGA) hardware in future research. The parameters of each layer of the proposed CTFNNC can be converted to the FPGA for verification.

References

1 S. Yin, X. W. Li, H. J. Gao, and O. Kaynak: IEEE Trans. Ind. Electron. **62** (2015) 657. https://doi.org/10.1109/TIE.2014.2308133
2 X. Chen, R. Yan, and Y. Liu: IEEE Instrum. Meas. Mag. **19** (2016) 22. https://doi.org/10.1109/MIM.2016.7462789
3 R. B. Randall and J. Antoni: Mech. Syst. Signal Process. **25** (2011) 485. https://doi.org/10.1016/j.ymssp.2010.07.017
4 J. Lee, F. Wu, W. Zhao, M. Ghaffari, L. Liao, and D. Siegel: Mech. Syst. Signal Process. **42** (2014) 314. https://doi.org/10.1016/j.ymssp.2013.06.004
5 Q. Zhu, Y. Qiao, N. Wu, and Y. Hou: IEEE/CAA J. Automatica Sinica **7** (2020) 597. https://doi.org/10.1109/JAS.2020.1003069
6 W. Liu, Z. Wang, Y. Yuan, N. Zeng, K. Hone, and X. Liu: IEEE Trans. Cybern. **51** (2021) 1085. https://doi.org/10.1109/TCYB.2019.2925015
7 D. Yu, J. Cheng, and Y. Yang: Mech. Syst. Signal Process. **19** (2005) 259. https://doi.org/10.1016/S0888-3270(03)00099-2
8 W. Guo and P. W. Tse: J. Sound Vibrat. **332** (2013) 423. https://doi.org/10.1016/j.jsv.2012.08.017
9 L. Saidi, J. B. Ali, and F. Fnaiech: ISA Trans. **53** (2014) 1650. https://doi.org/10.1016/j.isatra.2014.06.002
10 X. Qiu, Y. Ren, P. N. Suganthan, and G. A. J. Amaratunga: Appl. Soft Comput. **54** (2017) 246. https://doi.org/10.1016/j.asoc.2017.01.015
11 S. Park, S. Kim, and J. H. Choi: Mech. Syst. Signal Process. **108** (2018) 262. https://doi.org/10.1016/j.ymssp.2018.02.028
12 Y. Cheng, Z. W. Wang, B. Y. Chen, W. H. Zhang, and G. H. Huang: ISA Trans. **91** (2019) 218. https://doi.org/10.1016/j.isatra.2019.01.038
13 G. Goddu, B. Li, M. Y. Chow, and J. C. Hung: IECON '98 Proc. 24th Annu. Conf. IEEE Industrial Electronics Society (Cat. No.98CH36200) 1961–1965.
14 F. Bin and X. Wenbo: Comput. Chem. Eng **23** (2006) 343. https://doi.org/10.16866/j.com.app.chem2006.04.012
15 X. Wang, C. Wang, K. Zhu, and X. Zhao: Symmetry **15** (2002) 83. https://doi.org/10.3390/sym15010083
16 A. B. Patil, J. A. Gaikwad, and J. V. Kulkarni: 2016 2nd Int. Conf. Applied and Theoretical Computing and Communication Technology (iCATccT) 399–405.
17 J. Gai and Y. Hu: Shock. Vib. **2018** (2018) 8218657. https://doi.org/10.1155/2018/8218657
18 M. Wang, Y. Chen, X. Zhang, T. K. Chau, H. H. C. Iu, T. Fernando, Z. Li, and M. Ma: J. Vib. Eng. Technol. **10** (2022) 853. https://doi.org/10.1007/s42417-021-00414-7
19 D. T. Hoang and H. J. Kang: Neurocomputing **335** (2019) 327. https://doi.org/10.1016/j.neucom.2018.06.078

20 L. Zhou, C. Zhang, F. Liu, Z. Qiu, and Y. He: Comprehensive Rev. Food Sci. Food Saf. **18** (2019) 1793. https://doi.org/10.1111/1541-4337.12492
21 S. Li, G. Xie, W. Ji, X. Hei, and W. Chen: 2020 IEEE 9th Data Driven Control and Learning Systems Conf. (DDCLS) 117–122.
22 X. Wang, D. Mao, and X. Li: Measurement **173** (2021) 108518. https://doi.org/10.1016/j.measurement.2020.108518
23 C. J. Lin and J. Y. Jhang: Mathematics **9** (2021) 1502. https://doi.org/10.3390/math9131502
24 M. J. Hasan, M. Sohaib, and J. M. Kim: Computational Intelligence in Information Systems, CIIS 2018, Advances in Intelligent Systems and Computing 888 (Springer, Cham, 2019).
25 I. Goodfellow, Y. Bengio, and A. Courville: Deep Learning, Cambridge, MA, USA (MIT Press, Cambridge, 2016).
26 Z. Deng, Y. Jiang, F. Chung, H. Ishibuchi, and S. Wang: IEEE Trans. Fuzzy Syst. **21** (2013) 597. https://doi.org/10.1109/TFUZZ.2012.2212444
27 S. Zhang, S. Zhang, B. Wang, and T. G. Habetler: IEEE Access **8** (2020) 29857. https://doi.org/10.1109/ACCESS.2020.2972859
28 Case Western Reserve University (CWRU) Bearing Data Center: https://csegroups.case.edu/bearingdatacenter/pages/welcome-case-western-reserve-university-bearing-data-center-website (accessed July 2022).
29 J. Lee, H. Qiu, G. Yu, and J. Lin (2007): Rexnord Technical Services, IMS, University of Cincinnati, "Bearing Data Set", NASA Ames Prognostics Data Repository, NASA Ames Research Center, Moffett Field, CA, USA. http://ti.arc.nasa.gov/project/prognostic-data-repository (accessed December 2022).
30 Paderborn University, Bearing Data Center: https://mb.uni-paderborn.de/kat/forschung/datacenter/bearing-datacenter/ (accessed June 2022).
31 IEEE PHM 2012 Data Challenge Bearing Dataset: https://github.com/wkzs111/phm-ieee-2012-data-challenge-dataset (accessed July 2022).
32 H. Qiu, J. Lee, J. Lin, and G. Yu: J. Sound Vibrat. **289** (2006) 1066. https://doi.org/10.1016/j.jsv.2005.03.007
33 W. A. Smith and R. B. Randall: Mech. Syst. Signal Process. **64**–**65** (2015) 100. https://doi.org/10.1016/j.ymssp.2015.04.021
34 J. Chang: 7th World Congr. Intelligent Control and Automation (2008) 2454–2459.
35 H. Ogi, H. Tanaka, Y. Akimoto, and Y. Izui: Proc. 1st Int. Forum on Applications of Neural Networks to Power Systems (1991) 112–116.
36 S. Li, G. Xie, W. Ji, X. Hei, and W. Chen: IEEE 9th Data Driven Control and Learning Systems Conf. (DDCLS, 2020) 117–122.
37 C. J. Lin and J. Y. Jhang: IEEE Access **10** (2022) 14120. https://doi.org/10.1109/ACCESS.2022.3147866
38 T. Lu, F. Yu, C. Xue, and B. Han: J. Food Eng. **288** (2021) 110220. https://doi.org/10.1016/j.jfoodeng.2020.110220

About the Authors

Jyun-Yu Jhang received his B.S. and M.S. degrees from the Department of Computer Science and Information Engineering, National Chin-Yi University of Technology, Taichung, Taiwan, in 2013 and 2015, respectively, and his Ph.D. degree from the Institute of Electrical and Control Engineering in 2021. Currently, he is an assistant professor of the Department of Computer Science & Information Engineering, National Taichung University of Science and Technology, Taichung, Taiwan. His current research interests include fuzzy logic theory, type-2 neural fuzzy systems, evolutionary computation, machine learning, computer vision, and their applications. (jyjhang@nutc.edu.tw)

Cheng-Jian Lin received his B.S. degree in electrical engineering from Ta Tung Institute of Technology, Taipei, Taiwan, R.O.C., in 1986 and his M.S. and Ph.D. degrees in electrical and control engineering from National Chiao Tung University, Taiwan, R.O.C., in 1991 and 1996, respectively. Currently, he is a chair professor of the Computer Science and Information Engineering Department, National Chin-Yi University of Technology, Taichung, Taiwan, R.O.C., and dean of Intelligence College, National Taichung University of Science and Technology, Taichung, Taiwan, R.O.C. His current research interests are machine learning, pattern recognition, intelligent control, image processing, intelligent manufacturing, and evolutionary robots.
(cjlin@ncut.edu.tw)

Su-Wei Kuo received his B.S. degree from the Department of Electronic and. Computer Engineering, National Chin-Yi University of Technology, Taichung, Taiwan, in 2022. He is currently pursuing his M.S. degree with the Department of Computer Science & Information Engineering, National Chin-Yi University of Technology, Taichung, Taiwan. His current research interests include bearing fault diagnosis systems, deep learning, and neural fuzzy systems.
(pijh.s70210@gmail.com)